Fault feature extraction for rolling element bearing diagnosis based on a multi-stage noise reduction method

Junchao Guo[1], Dong Zhen[1,*], Haiyang Li[2], Zhanqun Shi[1], Fengshou Gu[2], Andrew. D. Ball[2]

[1]School of Mechanical Engineering, Hebei University of Technology, Tianjin, 300401, China.

[2]Centre for Efficiency and Performance Engineering, University of Huddersfield, Huddersfield, HD1 3DH, UK.

[*]Corresponding author: Tel: +86-22-26582598. E-mail address: d.zhen@hebut.edu.cn

Abstract

To extract impulsive feature from vibration signals with strong background noise and interference components for accurate bearing diagnostics., a multi-stage noise reduction method is proposed based on ensemble empirical mode decomposition (EEMD), wavelet denoising and modulation signal bispectrum (MSB) Firstly, noisy vibration signals are applied with EEMD to obtain a list of intrinsic mode functions (IMFs) that leverage the desired modulation components to different degrees. Then, a number of initial IMFs in the high frequency range, which are separated by using the mean of the standardized accumulated modes (MSAM) to have more modulation contents, are further denoised by a wavelet shrinkage approach. These cleaned IFMs in the high frequency are combined with the low frequency IFMs to construct a pre-denoised signal that maintains the modulation properties of the signal. Finally, a modulation signal bispectrum (MSB) is used to extract the modulation signature by suppressing further the residual random noise and deterministic interference components. This multiple stage noise reduction method is validated through a simulation study and two experimental fault cases studies of rolling element bearing. The results are more accurate and reliable in diagnosing the inner and outer race defects in comparison with the individual use of the start of the art EEMD or MSB.

The MSAM is taken as a novel criterion to divide the IMFs into low- and high-frequency parts. Subsequently, a wavelet based pre-denoising is used to process the high-frequency IMFs, which is then joined with the low-frequency IMFs to generate a reconstructed signal with much less noise. The EEMD-Wavelet model can effectively reduce the background noise and enhance the impulse characteristic in the vibration signal. However, the nonlinear modulation and uncoupling frequency components are still existed in the reconstructed signal. Finally, the modulation signal bispectrum (MSB) is explored to decompose the modulated components and extract the fault-related characteristics from the reconstructed signal.

The proposed method is validated through a simulation study and two experimental fault cases studies of rolling element bearing. The analysis results demonstrate that the proposed method is effective in the fault feature extraction with high accuracy in comparison with the individual EEMD and MSB.

Keywords: EEMD-Wavelet model; mean of the standardized accumulated modes; modulation signal bispectrum; rolling element bearing; feature extraction

1. Introduction

Rolling element bearings are important rotating parts in mechanical equipment but malfunctions may hinder the normal operation of the entire rotating machine [1]. Hence, the effective detection of the early damage stages of bearings has attracted much attention recently. In practical engineering, a series of impulse components will be generated when a rolling element bearing has a local defect [2]. However, these impulses are usually submerged in the complicated vibration signals that contain strong background noise and interference components, making the fault feature extraction extremely complicated and difficult [3]. Therefore, how to accurately extract impulsive feature from strong background noise and interference components is worthy for further study.

Up to now, various feature extraction approaches have been widely applied in rolling element bearing fault diagnosis [4-5]. For example, wavelet transform (WT), Wigner-Ville distribution (WVD), morphological filter (MF), and sparse decomposition, etc. Although these approaches have been widely certified in the bearing fault detection, they have their own unique disadvantages. For instance, the WT is a state-of-the-art analysis method, but its wavelet basis and mother wavelet need to be selected in advance [6-7]. The WVD is affected by cross-interference items [8-9]. The MF is well known for it can reserve signal details, but it suffers from the structure element selection problems [10-11]. The sparse decomposition has good signal decomposition performance, but it relies on the atom library and decomposition method [12-13]. However, these methods are not suitable to deal with complicated vibration signals that reflect nonlinear and non-stationary characteristics, while empirical mode decomposition (EMD) is not governed by this limitation because of its adaptive ability [14]. EMD is able to decompose a signal into a battery of intrinsic mode functions (IMFs). However, the end effects and mode mixing of EMD may lead to the IMFs losing its specific physical meaning.

Ensemble empirical mode decomposition (EEMD), a strengthened approach of EMD, is proposed by Wu and Huang [15] and it is able to eliminate the troubles of the EMD end effects and mode mixing by adding a finite white series to the measured data. Therefore, EEMD has obtained a lot of attentions in the field of rotating machinery fault diagnosis [16–18]. Cheng et al. combined EEMD and kernel principal component analysis (KPCA) to identify the extent of planetary gear failure damage [16]. Wang et al. applied EEMD to improved tunable Q-factor wavelet transform (TQWT) to well extract fault feature of rolling element bearings [17]. Žvokelj et al. proposed a multivariate analysis method based on EEMD and independent component analysis (ICA) for rolling element bearing fault detection and diagnosis [18]. The above-mentioned studies demonstrated that the EEMD can reduce background noise to improve the signal quality for extract fault feature effectively. However, how to select fault-sensitive IMFs components is still an inextricable problem. Recently a few analysis methods for the fault-sensitive IMFs selection have been reported. Lei et al. recommended correlation coefficient criterion to locate the optimal IMFs [19]. Xue et al. proposed the kurtosis criterion to select fault-sensitive IMFs [20]. Singh et al. used Jensen Rényi divergence (JRD) to search the optimal IMFs [21]. Hoseinzadeh et al. proposed the combined mutual information coefficient and energy to choose the IMFs [22]. However, these studies only concentrate upon analyzing few individual IMFs to extract fault-related characteristics, few researches pay attentions to reveal fault-related characteristics by considering the contribution of all IMFs to fault features extraction as different IMFs display different degrees of effectiveness in revealing fault characteristics [23-24]. Moreover, even EEMD can denoise and improve the signal to noise ratio (SNR) of the examined signal, there are still exist frequency coupling and nonlinear modulation components in the signal after EEMD analysis.

The modulation signal bispectrum (MSB) has emerged in the work of nonlinear feature extraction, because it allows efficient use of the modulation characteristics and detection coupling frequency pairs [25-27]. Gu et al. explored a novel approach for accurately breaking the rotor bar detection by a means of the MSB based motor current signal analysis (MCSA) [25]. Tian et al. proved that the MSB-based analysis approach can generate more accurate and stronger detection results for rolling element bearing fault diagnosis [26]. Guo et al. proposed a new approach combining wavelet packet energy (WPE) and MSB to detect planetary gearboxes faults [27]. The above-mentioned studies confirmed that the MSB is effective in demodulating a signal with modulation characteristics buried in strong noise and detecting coupling frequency pairs of a signal. However, the MSB exposes its weakness when processing the non-stationary vibration signal [24]. In addition, the frequency implementation of MSB can restrict its noise suppression capability due to the effect of spectral smearing.

To overcome the shortages respective to EEMD and MSB, a hybrid analysis method based on EEMD-Wavelet model and MSB for rolling element bearings fault diagnosis is proposed. EEMD is a typical adaptive time-frequency approach and plays a successful role in fault detection. To further improve the SNR of the vibration signal and take advantage of the contribution of all IMFs to fault feature extraction, this paper proposes the mean of the standardized accumulated modes (MSAM) to divide IMFs into low- and high-frequency IMFs. The high-frequency IMFs are denoised using a wavelet threshold and then reconstructed with the low-frequency IMFs to generate a reconstructed signal with more higher SNR. The MSB is then explored in terms of demodulating the reconstructed signal to extract fault-related characteristics.

The remainder of the paper is organized as follows. Section 2 describes the EEMD−Wavelet model. Section 3 presents the principles of the MSB. Section 4 introduces the detailed procedure of the proposed method based on simulation study. The EEMD-Wavelet-MSB is further tested to diagnose the rolling element bearings with inner and outer race faults in section 5. And the conclusions are presented in section 6.

2. Ensemble empirical mode decomposition (EEMD)-Wavelet model

2.1 EEMD

EMD is a self-adaptive approach to decompose a non-stationary and non-linear signal into a series instinct signal components namely instinct mode function (IMF) for more detailed analysis. As original EMD suffers from end effects and mode mixing problems, new noise-assisted data analysis variant, EEMD is often used. To understand its usefulness of EEMD in analyzing noise bearing signals, its implementation is outlined as follows [28]:

(1) Initialize the number of ensembles m and the added white noise amplitude A, with $i = 1$.

(2) Acquire the original signal $y_i(t)$ by increasing white noise $n_i(t)$ with amplitude A to the raw signal $y(t)$:

$$y_i(t) = y(t) + n_i(t) \tag{1}$$

(3) Apply the EMD method to decompose the original signal $y_i(t)$ into IMFs:

$$y_i(t) = \sum_{j=1}^{N} c_{i,j}(t) + r_{i,N}(t) \tag{2}$$

where $c_{i,j}(t)$ $(j = 1, 2, \dots, N)$ indicates the j-th IMF of the i-th trial, $i = 1,2, \dots, m$. and N is the number of IMFs.

(4) Repeat steps of (2) and (3) for m trials, with a finite white noise series n_i each time to acquire an ensemble of IMFs:

$$[c_{1,j}(t), c_{2,j}(t), \dots, c_{m,j}(t)] \tag{3}$$

(5) Counted the ensemble means of the corresponding IMFs as the end result:

$$c_j(t) = \frac{1}{m}\sum_{i=1}^{m} c_{i,j}(t) \tag{4}$$

where $c_j(t)$ indicates the *j-th* IMF decomposed by EEMD.

Additionally, the amplitude of the increased white noise A and the number of trials m in the ensemble are two critical parameters for the EEMD analysis. The final standard deviation of the error ε adopted by the increased white noise on the EEMD decomposition result is described as follow:

$$\varepsilon = A/\sqrt{m} \tag{5}$$

where A indicates 0.2 times the standard deviation of the signal, m presents 100, as suggested in Ref. [15.

It can be seen that EMD is essentially breaks a complicated down into a number of amplitude and frequency modulated (AM/FM) zero-mean MFs. In this way the modulation components induced by bearing fault can be more enhanced, which means that the random noise components are suppressed.

2.2 EEMD-Wavelet model

After applying EEMD for multi-scale decomposition of the signal, the criterion of the scale selection based on the mean of standardized accumulated modes (MSAM) is applied to distinguish high-frequency IMFs from a limited series of IMFs. The definition of MASM can be expressed as [29]:

$$\hat{h}_m = mean\left[\sum_{j=1}^{m}\left[c_j(t) - \frac{mean(c_j(t))}{std(c_j(t))}\right]\right] \qquad m \ll N \tag{6}$$

If $\hat{h}_m$ deviates from zero, the scale m is defined as the sign to discriminate between the high-frequency and the low-frequency IMFs.

In addition, in order to eliminate noise in high-frequency IMFs for further improvement of SNR, the wavelet threshold (WT) is employed due to its ability of separating signals and noise referred to [30]. During the processing of the WT, the Daubechies (db10) is selected as the mother wavelet because of the Daubechies family is most similar to the vibration signal of the rolling element bearing [31]. The wavelet coefficients $\bar{c}_j$ given with the hard-threshold and soft-threshold functions are expressed as in reference [32]:

Hard-threshold function:

$$\bar{c}_j = \begin{cases} c_j & |c_j| \gg T \\ 0 & |c_j| < T \end{cases} \tag{7}$$

Soft-threshold function:

$$\bar{c}_j = \begin{cases} sign(c_j)(|c_j| - T) & |c_j| \gg T \\ 0 & |c_j| < T \end{cases} \tag{8}$$

where $T = \sigma\sqrt{2InN}$ is the universal threshold, σ and N are the standard deviation of the noise and the length of the signal. Compared with the hard-threshold function, the soft-threshold function can obtain better results for processing the denoised signal [33]. Hence, the soft-threshold function is employed in the proposed method. In addition, the soft-threshold noise reduction can effectively maintain the integrity of useful signals [34]. The resulting signal is expressed as:

$$\tilde{y}(t) = \sum_{j=1}^{m-1}\bar{c}_j(t) + \sum_{j=m}^{N} c_j(t) + r_{i,N}(t) \tag{9}$$

where $\bar{c}_j$ are the de-noised high-frequency IMFs by WT.

The scheme of EEMD-Wavelet model can be illustrated as Fig.1.

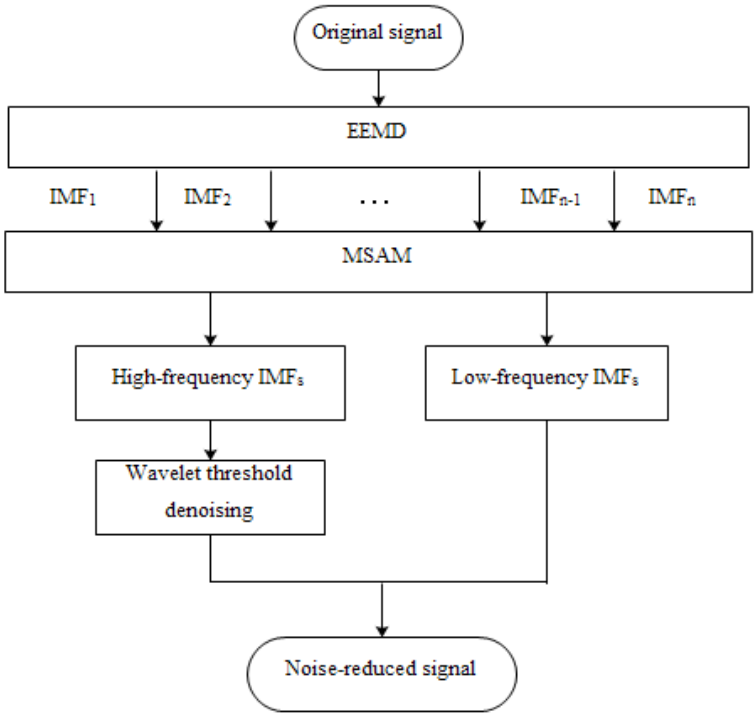

Fig.1. The flowchart of the EEMD-Wavelet model

3. Modulation Signal Bispectrum

3.1 A description of MSB method

MSB is a promising analysis method based on the improvement of the conventional bispectrum [25]. It has the merits of suppressing uncoupling frequency components and demodulating modulation components for rotating machinery fault diagnosis [25-27]. For a discrete-time signal $x(t)$ with corresponding discrete Fourier transform $X(f)$, the MSB can be expressed in the frequency domain as [26]:

$$B_{MS}(f_c, f_x) = E < X(f_c + f_x)X(f_c - f_x)X^*(f_c)X^*(f_c) > \quad (10)$$

where $B_{MS}(f_c, f_x)$ and $E <>$ are the bispectrum of signal $x(t)$ and expectation operator. The f_c and f_x indicate the carrier frequency and modulating frequency, $(f_c + f_x)$ and $(f_c - f_x)$ are the higher and lower sideband frequencies, respectively.

The overall phase of the MSB can be expressed as:

$$\emptyset_{MS}(f_c, f_x) = \emptyset(f_c + f_x) + \emptyset(f_c - f_x) - \emptyset(f_c) - \emptyset(f_x) \quad (11)$$

When the two components f_c and f_x are coupled, their phases are related as follows:

$$\begin{cases} \emptyset(f_c + f_x) = \emptyset(f_c) + \emptyset(f_x) \\ \emptyset(f_c - f_x) = \emptyset(f_c) - \emptyset(f_x) \end{cases} \quad (12)$$

The substitution of Eq. (12) into Eq. (11) demonstrates that the whole phase of the MSB is zero and the MSB amplitude is determined by the product of the four dimensions. Thus, a bispectral peak appears at bifrequency (f_c, f_x) that considering the two sidebands simultaneously. By contrast, the noise exhibits random phases and their amplitude can be suppressed by the expectation average over MSB sets from different signal segments. These effects then provide a more accurate and effective representation of the modulation characteristics in noisy signals.

To quantify the sideband amplitude more exactly, MSB is improved by eliminating the influence of f_c using magnitude normalization. The MSB sideband estimator (MSB-SE) is denoted by [27]:

$$B_{MS}^{SE}(f_c, f_x) = \frac{B_{MS}(f_c,f_x)}{\sqrt{|B_{MS}(f_c,0)|}} \tag{13}$$

where $B_{MS}(f_c, 0)$ indicates the squared power spectrum estimation at $f_x = 0$.

A typical analysis result of MSB-SE can be presented as Fig. 2.

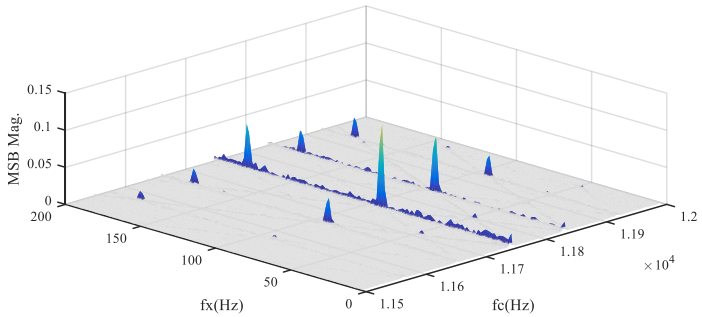

Fig.2. The result of the MSB-SE

3.2 An MSB detector

According to the analysis results of MSB-SE as shown in Fig.2, the optimal carrier frequency range to diagnose the bearing fault is at a given value of f_c and can be referred to as f_c^{best}, which indicates a maximum B_{MS}^{SE} peak. To get suboptimal f_c slices, $B_{MS}^{SE}(f_c^n, f_x)$ can be expressed as the compound MSB slice $\mathrm{B}(f_c)$ as shown in Fig.3, which is counted by averaging the main MSB peaks in the incremental orientation of the f_x [26]:

$$\mathrm{B}(f_c) = \frac{1}{M-1}\sum_{m=2}^{M} B_{MS}^{SE}\left(f_c, m\Delta f\right) \tag{14}$$

where Δf indicates the frequency resolution in the f_x orientation.

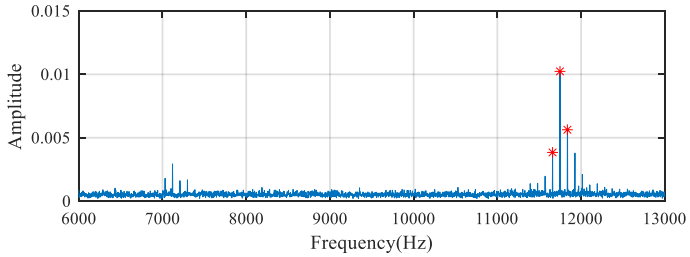

Fig.3. The compound MSB slice $\mathrm{B}(f_c)$

To obtain results that are more robust, the MSB modulation detector is improved using the average of a few suboptimal MSB slices in Fig.3 as marked with '*' and can be expressed in Eq. (15):

$$\mathrm{B}(f_x) = \frac{1}{N}\sum_{n=1}^{N} B_{MS}^{SE}(f_c^n, f_x)\ (f_x > 0) \tag{15}$$

where N presents the total number of selected f_c suboptimal slices (3, in the case of Fig.2), which depends on the importance of the peaks themselves. The MSB detector is shown in Fig. 4.

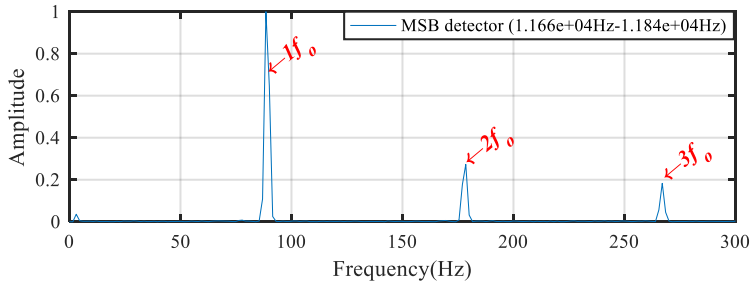

Fig.4. Results of the MSB detector

4. The proposed fault feature extraction method

4.1 The procedure of the proposed method

Motivated by the advantages of the EEMD-Wavelet model and MSB, this paper proposed an EEMD-Wavelet-MSB method for fault feature extraction of rolling element bearing. The basic idea of the EEMD-Wavelet-MSB is illustrated in Fig. 5 and the work is achieved by carrying out the following several steps:

(1) Decompose the raw signal into a few series of IMFs using EEMD.

(2) Calculate the MSAM value of different decomposition levels of EEMD.

(3) Judge the MSAM value in the step (2). If the MSAM value significantly deviates from zero at the m-th scale, the IMFs before the m-th scale are considered to be high-frequency and the rest IMFs are at low-frequency.

(4) Denoise the high-frequency IMFs using wavelet threshold, which is then combined with the low-frequency IMFs to produce the reconstructed signal.

(5) Extract the fault-related characteristics by applying the MSB to the reconstructed signal.

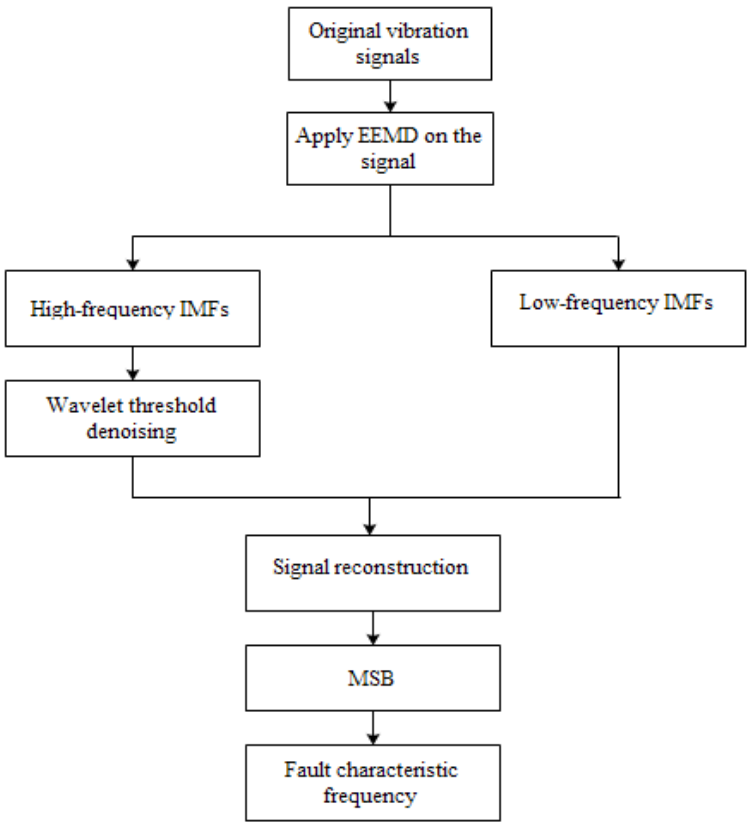

Fig.5. The flowchart of EEMD-Wavelet-MSB

4.2 Simulated signal analysis

To validate the effectiveness of the EEMD-Wavelet-MSB, a simulated vibration signal $x(t)$ for outer race fault of rolling element bearing is expressed as follows [26]:

$$\begin{cases} x(t) = \sum_{m=-N}^{N} A_m(t_i)\, e^{-\alpha(t_i)} \cos(w_r t_i)\, u(t_i) + n(t) \\ t_i = t - (m/f_0) \end{cases} \tag{16}$$

where A_m represents the amplitude of the m^{th} fault impulse signal, N stands the number of impulse, $f_0 = 88.5$ Hz indicates the fault characteristic frequency, α and w_r are the structural damping characteristic and aroused resonance frequency, $u(t)$ stands a unite step function, $n(t)$ is typical Gaussian white noise with a SNR of -7.14 dB.

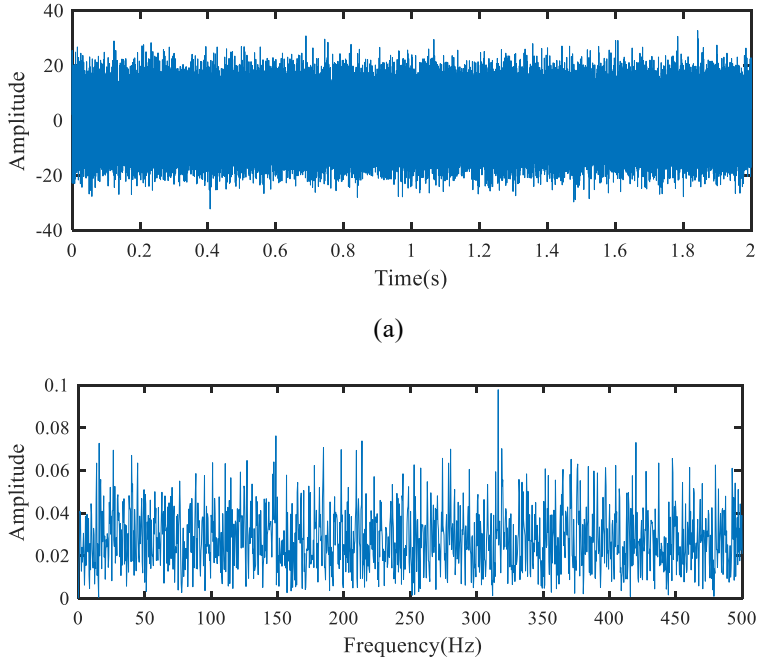

(a)

(b)

Fig. 6. Simulated fault signal of bearing outer race: (a) waveform (b) spectrum

Fig. 6 shows the waveform and corresponding spectrum of the simulated bearing fault signal. The fault components cannot be revealed from the spectrum in Fig. 6(b) due to the weak impulsive feature is merged with strong background noise. The signal is then decomposed into 18 IMFs by EEMD as shown in Fig.7.

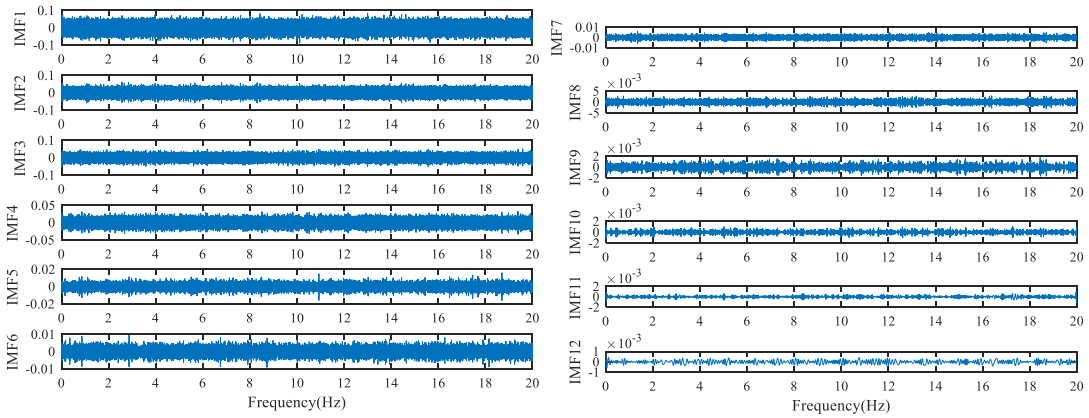

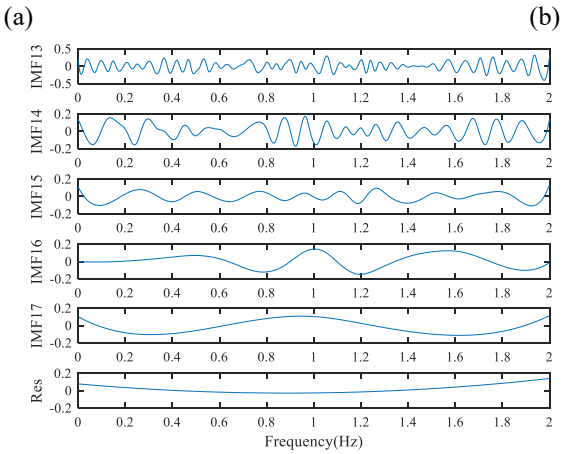

Fig.7. The IMFs decomposed by EEMD for the simulated signal:
(a) IMF1–IMF6 (b) IMF7–IMF12 (c) IMF13–IMF17 and one residual.

To accurately divide the IMFs, the MSAM is applied to divide the IMFs into low- and high-frequency parts. The relationship between the MSAM and scale is shown in Fig. 8. It shows that the appropriate scale for discriminating high-frequency from low-frequency IMFs is at 7 as calculated using Eq.(6). The high-frequency IMFs (from IMF1 to IMF6) is denoised by WT, the low-frequency IMFs (from IMF7 to IMF18 includes the residual signal) and the denoised high-frequency IMFs are then combined to produce the reconstructed signal.

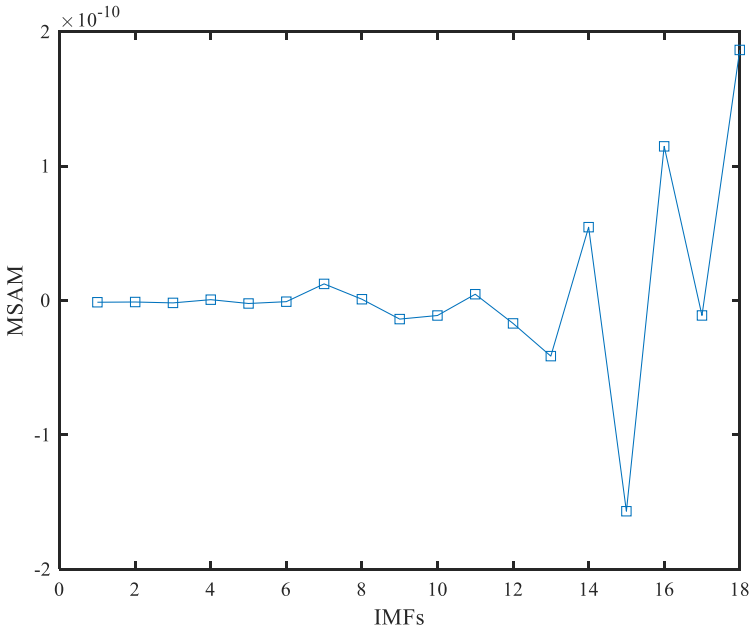

Fig.8. Relationship between the scale and MSAM

The MSB is applied to analyze the reconstructed signal to decompose the modulated components. The steps of calculating the MSB are as follows. Firstly, the MSB and sideband estimator are calculated using Eq. (10) and (13). Secondly, the MSB slice $B(f_c)$ is calculated using Eq. (14) and the suboptimal f_c slices are chosen in Fig. 9 (a). Finally, the MSB detector is calculated using Eq. (15) and the results are shown in Fig. 9 (b). It is clearly seen that the MSB detector can clearly identify the fault-related characteristic frequency and its harmonics. This indicates that the EEMD-Wavelet-MSB is capable of suppressing noise and decomposing the interference modulation components.

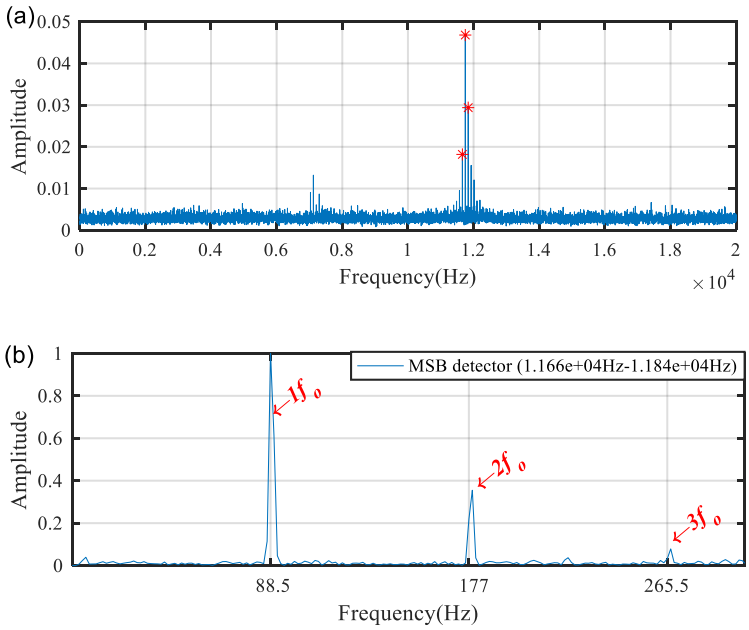

Fig.9. Analysis results of EEMD-Wavelet-MSB (a) MSB slice (b) MSB detector

5. Experimental verification

Two experimental cases were carried out to study the effectiveness of the EEMD-Wavelet-MSB for extracting the fault-related characteristic frequency. And the performance of the EEMD-Wavelet-MSB is compared with the individual EEMD and MSB during the experimental case studies.

5.1 Description of the Experiment

The test platform for fault diagnosis of rolling element bearing is shown in Fig.10. The test rig is consisted of an AC motor, a dynamic brake, two piezoelectric accelerometer sensors, supporting bearing as well as three flexible coupling. In the experiment, one piezoelectric accelerometer was mounted on the motor drive end bearing housing, and the other piezoelectric accelerometer was positioned on the bearing housing, which were used to collect the vibration signals. The data sampling frequency is 96 kHz and the data length are 1920000 points collected by YE62332B data acquisition system. The fault modes include an outer race fault was installed on the motor bearing and an inner race fault was set at the supporting bearing as illustrated in Fig. 11 (a) and (b), respectively. The kinematical parameters and fault-related characteristic frequency of the test bearings are listed in Table 1 and 2.

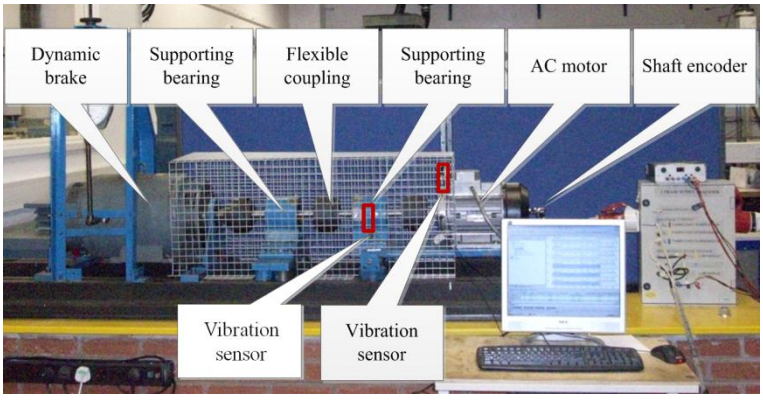

Fig.10. Rolling element bearing test platform

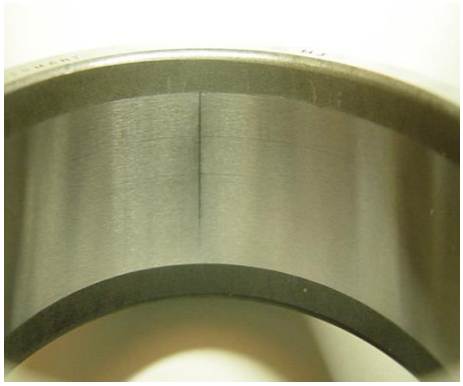

(a) (b)

Fig.11. The fault modes: (a) outer race fault (b) inner race fault

Table 1. Kinematical parameters of the test bearings

Bearing type	Ball numbers d (mm)	Pitch Diameter D_m (mm)	Ball Number z	Contact Angle β
6206ZZ	9.53	46.4	9	0°
6008	7.9	54	12	0°

Table 2. Fault-related characteristic frequency of the test bearings

Bearing type	Outer race f_o (Hz)	Inner race f_i (Hz)	Rolling element f_b (Hz)	Fundamental cage f_c (Hz)
6206ZZ	89.33	130.99	62.42	9.93
6008	49.25	65.17	33.60	4.10

5.2 Fault detection of the motor bearing outer race

Fig. 12 presents the waveform and its corresponding spectrum of the measured vibration signal of the test motor fault bearing. Obviously, the fault-related characteristic frequency f_o is fused by strong background noise and interference components as shown in Fig.12(b).

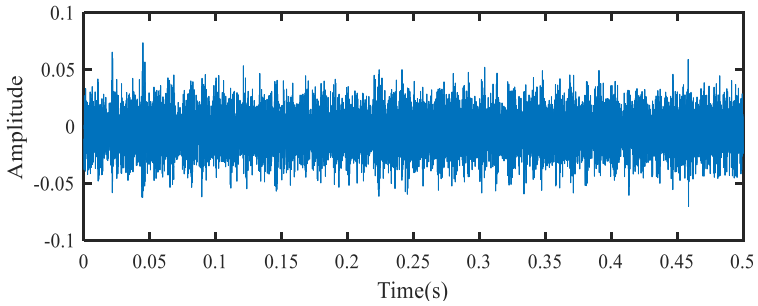

(a)

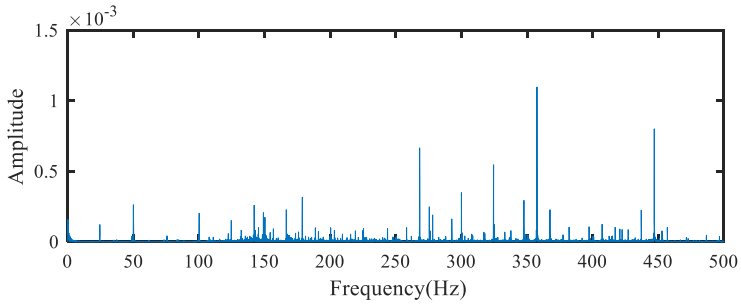

(b)

Fig.12. Measured vibration signal of motor fault bearing: (a) waveform (b) spectrum

The measured motor fault bearing vibration signal is first decomposed into 18 IMFs and one residual component by EEMD and the MSAM values are calculated then. Fig. 13 shows the relationship between the scale and MSAM. It is seen that the appropriate scale for discriminating of high-frequency and low-frequency IMFs is 10. The high-frequency IMF (from IMF1to IMF9) is denoised using the wavelet threshold, then the low-frequency IMFs (from IMF10 to IMF18 and one residual) and denoised high-frequency IMFs are reconstructed. The envelope analysis (EA) is employed to analyze the reconstructed signal, and the normalized EA result is given in Fig.14. There are many interference frequencies displayed around the fault-related characteristic frequency and its harmonics.

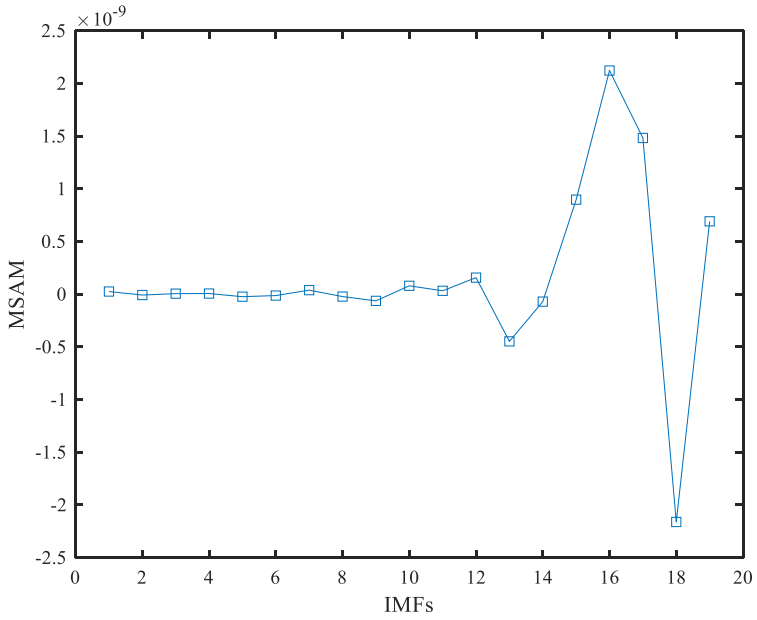

Fig.13. Relationship between the scale and MSAM.

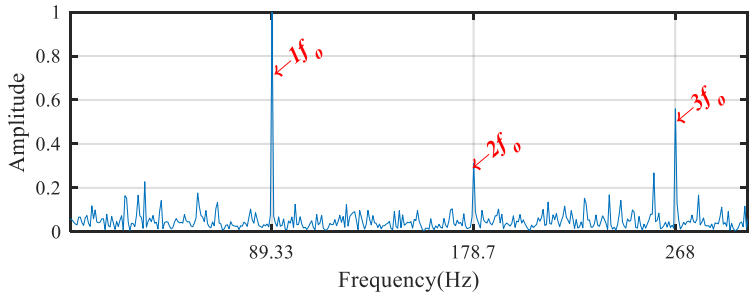

Fig.14. Envelope spectrum of the reconstruction signal

The MSB is then used to process the reconstructed signal to extract fault-related characteristic frequency, and the results are shown in Fig. 15. It can be seen that the MSB can clearly identify the fault-related characteristic frequency and its harmonics with lower interference noise. For comparative analysis, the individual MSB is used to analyze the measured vibration signals that are not processed by the EEMD-Wavelet model to extract fault-related characteristic frequency and the results are presented in Fig. 16. Although MSB analysis results can reveal the fault-related characteristic frequency and its harmonics, there are also some impulsive interference components, especially around the higher order harmonics. Moreover, the bandwidth is wider than the proposed method. This indicates that the EEMD-Wavelet-MSB receives more precise results in the fault feature extraction for rolling element bearing fault diagnosis.

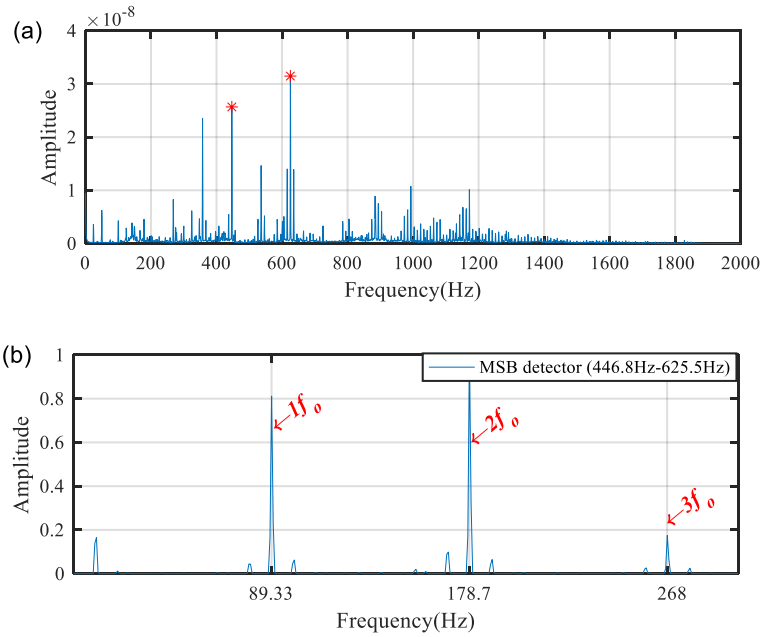

Fig.15. Analysis results of EEMD-Wavelet-MSB (a) MSB slice (b) MSB detector

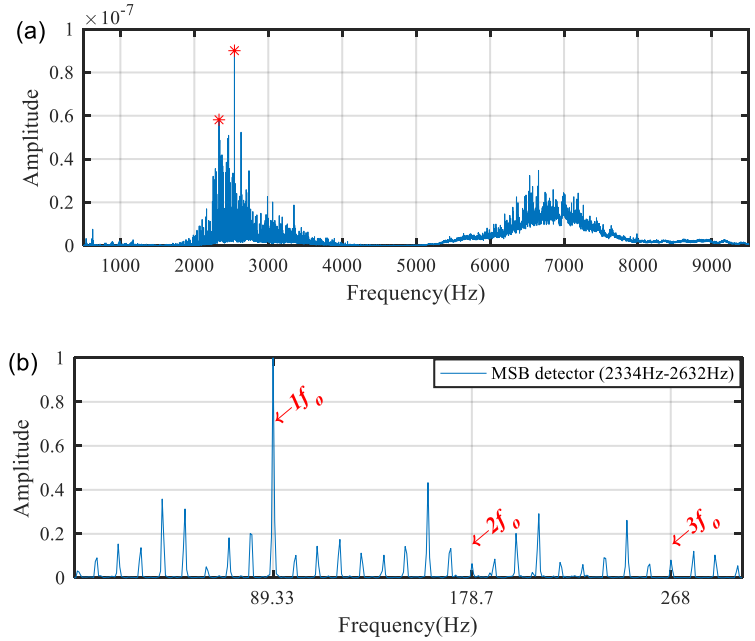

Fig.16. Analysis results of MSB (a) MSB slice (b) MSB detector

5.3 Fault detection of the supporting bearing inner race

Fig. 17 illustrates the waveform and spectrum of the measured vibration signal of the test supporting fault bearing. The fault-related characteristic frequency is obviously merged with heavy noise and difficult to be extracted based on the spectrum as shown in Fig.17(b).

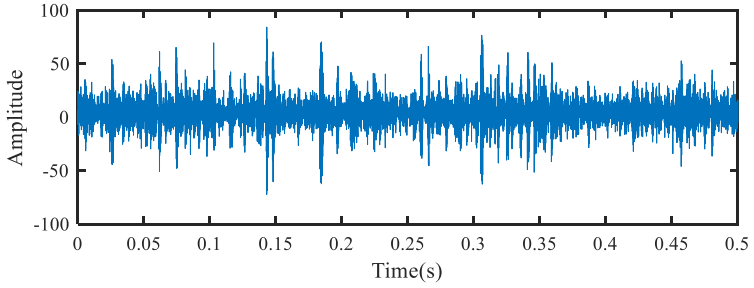

(a)

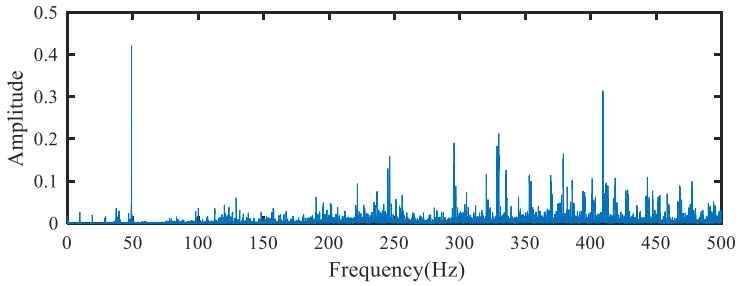

(b)

Fig.17. Measured vibration signal of supporting fault bearing : (a) waveform (b) spectrum

The supporting fault bearing vibration signal is initially decomposed into 19 IMFs and one residual component by EEMD and will not be shown in the present study. Fig. 18 shows the relationship between the scale and MSAM. It can be found that the appropriate scale for discriminating of low- and high-frequency IMFs is 10. The high-frequency IMF (from IMF1to IMF9) is denoised using the db 10 wavelet, then the low-frequency IMFs (from IMF10 to IMF18 and one residual) and denoised high-frequency IMFs are reconstructed. The normalized EA spectrum of the reconstructed signal is presented in Fig.19. It can extract the fault-related frequency and its harmonics， but they are mixed with much noise and the effect of interference components still exists as shown in Fig.19.

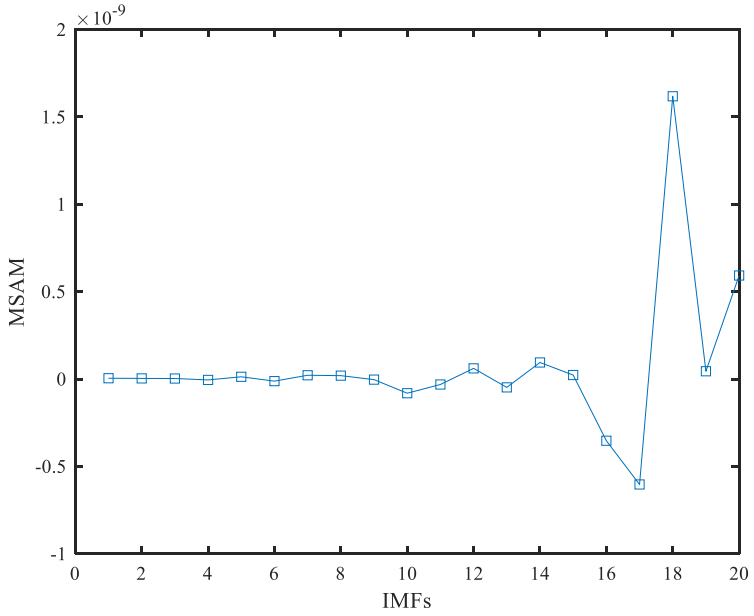

Fig.18. Relationship between the scale and MSAM

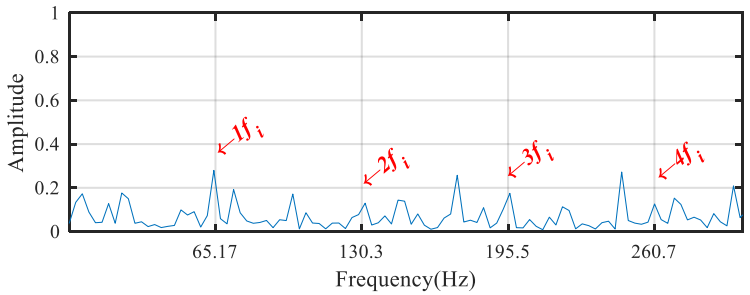

Fig.19. Envelope spectrum of the reconstruction signal

The MSB is then used to analyse the reconstructed signal to extract fault-related characteristic frequency, the results are shown in Fig. 20. It can be seen from Fig. 20 that the fault-related characteristic frequency and its harmonics are obvious. And the bandwidth of the EEMD-Wavelet-MSB is narrower than that of individual MSB analysis results as shown in Fig. 21. In contract, individual MSB analysis results are mixed with noise and interference components, especially around the higher order harmonics. This makes it difficult to extract fault features accurately. The comparative analysis indicate that the EEMD-Wavelet-MSB is a more effective and accurate fault feature extraction approach.

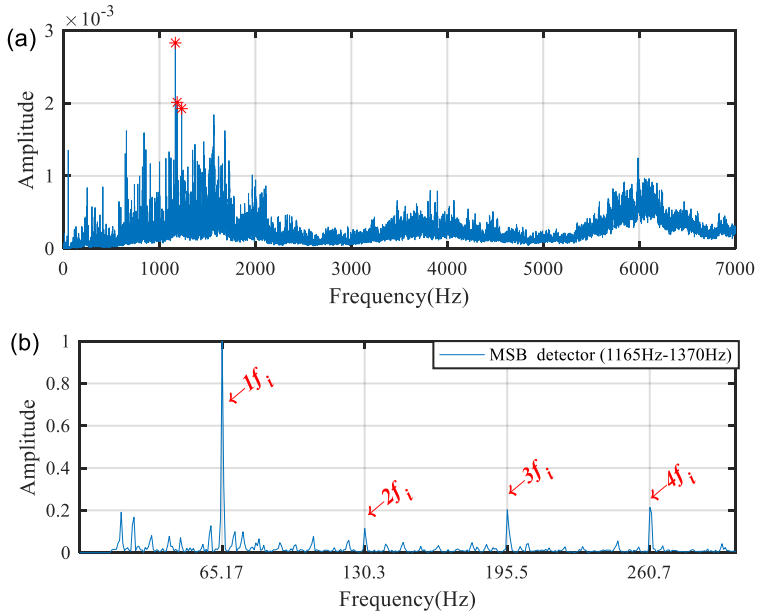

Fig.20. Analysis results of EEMD-Wavelet-MSB (a) MSB slice (b) MSB detector

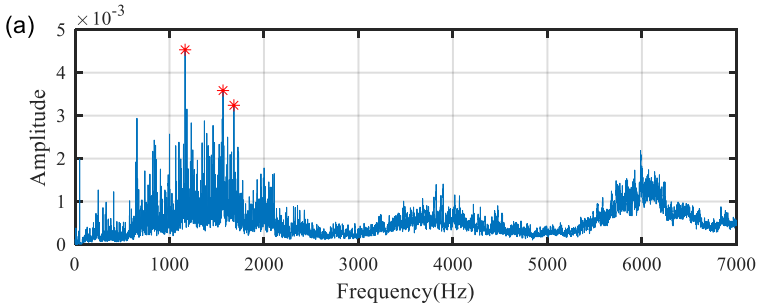

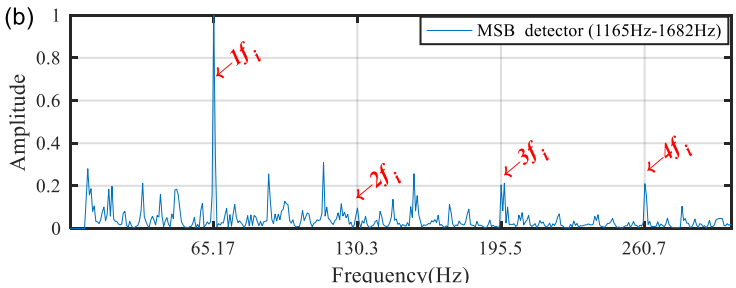

Fig.21. Analysis results of MSB (a) MSB slice (b) MSB detector

6. Conclusions

In this paper, a novel fault feature extraction approach based on EEMD-Wavelet model and MSB is proposed for rolling element bearing fault diagnosis. EEMD-Wavelet model is applied as a pre-filter to highlight the fault-related impulse components of the vibration signal through suppressing the background noise and utilizing the contribution of all IMFs to fault feature extraction. And then MSB is explored to extract the fault feature by demodulating the coupling frequency pairs and suppressing the uncoupling interference components. The performance and efficiency of the proposed method have been verified based on the simulation analysis and two fault diagnosis cases of the rolling element bearing inner and outer race. The analysis results show that the proposed method is efficient in the fault feature extraction with higher accuracy in comparison with the individual EEMD and MSB analysis. Especially the fault characteristic frequencies located in high order harmonics are better enhanced by EEMD-Wavelet-MSB. Moreover, the bandwidth of the EEMD-Wavelet-MSB for fault feature detection is about half the bandwidth of the individual MSB analysis. Therefore, it can be confirmed that the proposed method can be regarded as an efficient and accurate technique for fault feature extraction and diagnosis of rolling element bearing in early stage.

Acknowledgment

This research is supported by the National Natural Science Foundation of China (Grant no. 51605133; 51705127), Hebei Provincial International Science and Technology Cooperation Program of China (Grant no. 17394303D).

References

[1] Z. Feng, X. Chen, T. Wang. Time-varying demodulation analysis for rolling bearing fault diagnosis under variable speed conditions. J. Sound. Vib. 400 (2017) 71-85.

[2] X. Yan, M. Jia, W. Zhang, et al. Fault diagnosis of rolling element bearing using a new optimal scale morphology analysis method. Isa. T. 73 (2018) 165-180.

[3] Z. Meng, X. Zhan, J. Li et al. An enhancement denoising autoencoder for rolling bearing fault diagnosis. Measurement. 130 (2018) 448-454.

[4] Q. Zhang, J. Gao, H. Dong, et al. WPD and DE/BBO-RBFNN for Solution of Rolling Bearing Fault Diagnosis. Neurocomputing. 312 (2018) 27-33.

[5] H. Shao, H. Jiang, F. Wang, et al. Rolling bearing fault diagnosis using adaptive deep belief network with dual-tree complex wavelet packet. Isa. T. 69 (2017) 187-201.

[6] R. Shao, W. Hu, Y. Wang, et al. The fault feature extraction and classification of gear using principal component analysis and kernel principal component analysis based on the wavelet packet transform. Measurement. 54 (6) (2014) 118-132.

[7] Z. Liu, Z. He, W. Guo, et al. A hybrid fault diagnosis method based on second generation wavelet de-noising and local mean decomposition for rotating machinery. Isa. Transactions. 61 (2016) 211-220.
[8] R.B Pachori, A. Nishad. Cross-terms reduction in the Wigner–Ville distribution using tunable-Q wavelet transform. Signal Processing 120 (2016) 288-304.
[9] Y. Liu, J. Zhang, L. Ma. A fault diagnosis approach for diesel engines based on self-adaptive WVD, improved FCBF and PECOC-RVM. Neurocomputing 177 (2016) 600-611.
[10] F. Deng, S. Yang, G. Tang, et al. Self adaptive multi-scale morphology AVG-Hat filter and its application to fault feature extraction for wheel bearing. Meas. Sci. Technol. 28 (2017) 045011.
[11] Y. Li, X. Liang, M.J Zuo. A new strategy of using a time-varying structure element for mathematical morphological filtering. Measurement. 106 (2017) 53-65.
[12] Z. Feng, Y. Zhou, M. Zuo, et al. Atomic decomposition and sparse representation for complex signal analysis in machinery fault diagnosis: A review with examples. Measurement. 103 (2017) 106-132.
[13] X. Chen, Z. Du, J. Li, et al. Compressed sensing based on dictionary learning for extracting impulse components. Signal. Processing. 96 (5) (2014) 94-109.
[14] L. Wang, Z. Liu, Q. Miao, et al. Time-frequency analysis based on ensemble local mean decomposition and fast kurtogram for rotating machinery fault diagnosis. Mech. Syst. Sig. Process. 103 (2018) 60-75.
[15] Z. WU, N.E. Huang, et al. Ensemble empirical mode decomposition: a noise-assisted data analysis method. Advances in Adaptive Data Analysis 1 (2009) 1-41.
[16] G. Cheng, X. Chen, H. Li, et al. Study on planetary gear fault diagnosis based on entropy feature fusion of ensemble empirical mode decomposition. Measurement. 91 (2016) 140-154.
[17] H. Wang, J. Chen, G. Dong. Feature extraction of rolling bearing's early weak fault based on EEMD and tunable Q-factor wavelet transform. Mech. Syst. Sig. Process. 48 (2014) 103-119.
[18] M. Žvokelj, S. Zupan, I. Prebil. EEMD-based multiscale ICA method for slewing bearing fault detection and diagnosis. J. Sound. Vib. 370 (2016) 394-423.
[19] Y. Lei, M.J. Zuo. Fault diagnosis of rotating machinery using an improved HHT based on EEMD and sensitive IMFs. Meas. Sci. Technol. 20 (12) (2009) 125701.
[20] X. Xue, J. Zhou, Y. Xu, et al. An adaptively fast ensemble empirical mode decomposition method and its applications to rolling element bearing fault diagnosis. Mech. Syst. Sig. Process. 62–63 (2015) 444-459.
[21] J. Singh, A.K Darpe, S.P Singh. Bearing damage assessment using Jensen-Rényi Divergence based on EEMD. Mech. Syst. Sig. Process. 87 (2017) 307-339.
[22] M.S. Hoseinzadeh, S.E. Khadem, M.S. Sadooghi. Quantitative diagnosis for bearing faults by improving ensemble empirical mode decomposition. Isa. T. https: //doi.org/10.1016/j. isatra. 2018. 09. 008.
[23] P. Nguyen, J.M. Kim. Adaptive ECG denoising using genetic algorithm-based thresholding and ensemble empirical mode decomposition. Information Sciences. 373 (2016) 499-511.
[24] L. Saidi, J.B. Ali, F. Fnaiech. Bi-spectrum based-EMD applied to the non-stationary vibration signals for bearing faults diagnosis. Isa. T. 53 (2014) 1650-1660.
[25] F. Gu. T. Wang. A. Alwodai. et al., A new method of accurate broken rotor bar diagnosis based on modulation signal bispectrum analysis of motor current signals. Mech. Syst. Sig. Process. 50-51 (2015) 400-413.
[26] X. Tian, J.X Gu, I. Rehab, et al. A robust detector for rolling element bearing condition monitoring based on the modulation signal bispectrum and its performance evaluation against the Kurtogram. Mech.

Syst. Sig. Process. 100 (2018) 167-187.
[27] J. Guo, Z. Shi, H. Li, et al. Early fault diagnosis for planetary gearbox based wavelet packet energy and modulation signal bispectrum analysis. Sensors. 18 (2018) 2908.
[28] X. Xue, J. Zhou. A hybrid fault diagnosis approach based on mixed-domain state features for rotating machinery. Isa Trans. 66 (2017) 284-295.
[29] C. Liu, F. Zhou, Y. Liu. GPS/Pseudolites technology based on EMD-wavelet in the complex field conditions of mine. Procedia Earth and Planetary Science, 1 (2009) 1293-1300.
[30] Y. Zhang, J. Lian, F. Liu. An improved filtering method based on EEMD and wavelet-threshold for modal parameter identification of hydraulic structure. Mech. Syst. Sig. Process. 68-69 (2016) 316-329.
[31] Y. Wang, G. Xu, L. Liang, et al. Detection of weak transient signals based on wavelet packet transform and manifold learning for rolling element bearing fault diagnosis. Mech. Syst. Sig. Process, 54-55 (2015) 259-276.
[32] W. Wang, Q. Chen, D. Yan, et al. A novel comprehensive evaluation method of the draft tube pressure pulsation of Francis turbine based on EEMD and information entropy. Mech. Syst. Sig. Process, 116 (2019) 772-786.
[33] P. Nguyen, J.M Kim. Adaptive ECG denoising using genetic Algorithm-Based thresholding and ensemble empirical mode decomposition. Inform. Sciences, 373 (2016) 499-511.
[34] J. Chang, L. Zhu, H. Li, et al. Noise reduction in Lidar signal using correlation-based EMD combined with soft thresholding and roughness penalty. Opt. Commun, 407 (2018) 290-295.